Neural-Network based algorithm for ice concentration retrievals from satellite passive microwave data

Leonid P. Bobylev, *Member, IEEE*, Elizaveta V. Zabolotskikh, Leonid M. Mitnik, and Ola M. Johannessenn

***Abstract*—Present algorithms for observing the multiyear ice cover are not accurate in multiyear fraction calculations, which is a significant disadvantage of the present system of global ice monitoring considering the fact that multiyear ice is one of the key indicators of changes in the Arctic climate. In this research regionally differing Neural Networks (NN)-based algorithms for total and multiyear Arctic sea ice concentration retrievals from Special Sensor Microwave Imager (SSM/I) data are developed using closed scheme of the numerical experiment. Era-40 Reanalysis data on atmospheric parameter profiles and sea ice temperature are used for the numerical integration of the radiation transfer of the microwave emission in the Atmosphere-Ocean-Ice System. The data on cloud liquid water content and cloud boundaries are modeled basing on the results of Arctic SHEBA experiment. Numerical values for first year and multiyear ice emissivities are taken from published experimental data. The calculated radiometer brightness temperature values are used for NN-based theoretical algorithm development. New weather filter is defined. The algorithms are validated for stable winter conditions using collocated SSM/I data and Synthetic Aperture Radar (SAR) images, classified by an ice expert.**

***Index Terms*— multiyear ice concentration, satellite passive microwave, Arctic, Neural Networks, physical modeling.**

I. Introduction

Polar sea ice is a vital component of the global climate system because of its high albedo, its low heat conductivity which limits the exchange of heat between ocean and atmosphere, and its role in altering oceanic water mass properties and circulation. A long-term, large-scale characterization of the global sea ice cover is needed for sea ice trend studies and for climate model validation studies (Comiso and Parkinson, 2004). The most consistent source of such data continues to be satellite passive microwave sensors. Microwave sensors, not limited by weather conditions or light levels, are particularly well suited for monitoring sea ice, because of the strong contrast in thermal microwave emission between areas of ice-free ocean and ice-covered waters (Zwally et al.,1983).

The principal quantitative measure of the global sea ice cover is sea ice concentration. It is this parameter that continues to be produced routinely from satellite passive microwave systems for both global change research and operational requirements.

Starting from Scanning Multichannel Microwave Radiometer (SMMR), launched in 1978 with its multichannel capability, a number of algorithms appeared to derive sea ice concentrations (Svendsen et al., 1983; Swift et al., 1985). The various algorithms take advantage of two or more channels to reduce errors associated with physical temperature variability, emissivity anomalies, and weather effects.

In 1987, the first in a new series of passive microwave radiometers was launched as part of the Defense Meteorological Satellite Program (DMSP). Using these data, several new algorithm improvements have been made (e.g., Cavalieri, 1994; Comiso, 1995, Markus and Cavalieri, 2000). The key up-to-date problems of the passive microwave data inversion into sea ice concentration remain discrimination between various ice types and misinterpretation of the sea ice due to atmospheric influence.

In this research another approach is suggested for total and multiyear (MY) Arctic sea ice concentration retrievals from SSM/I data. Total ice concentration is considered as a sum of first year and MY ice concentrations. The retrieval algorithms are developed using closed scheme of the numerical experiment. and Neural Networks (NN) as an inversion function. Era-40 Reanalysis data on atmospheric parameter profiles and sea ice temperature are used for the numerical integration of the radiation transfer of the microwave emission in the Atmosphere-Ocean-Ice System. The data on cloud liquid water content and cloud boundaries are modeled basing on the results of Arctic SHEBA experiment. The ice emissivities are taken from published experimental data. The calculated radiometer brightness temperature values, summarized with simulated radiometric noise, are used for NN-based theoretical algorithm development. Weather filter, basing on numerical simulation of ice free system, is defined

The first validation results are obtained by means of comparison of NN- retrieved ice concentrations with Synthetic Aperture Radar (SAR) images, classified by an ice expert, under stable winter conditions with the absence of melting.

II. Methodology

A. Forward Problem Solution

The Forward problem solution consisted of the following steps: defining geophysical model of the system; determination of the models of microwave radiation-environmental medium interaction; and creation of the dataset of simultaneous meteorological, ocean and ice data for brightness temperature calculations;

978-1-4244-1987-6/08/$25.00 ©2008 IEEE

1) Radiative transfer modeling

Computer simulations of the radiometric brightness temperatures (BT) were carried out for the input data sets consisting of atmospheric, oceanic and ice data. These simulations were done for frequencies, polarization, sensitivity, spatial resolution and sensing geometry of SSM/I. The Atmosphere-Ocean-Ice System model was restricted by non-precipitating conditions, using absorption-emission approximation and neglecting microwave radiative scattering from large rain drops and ice particles. The general restriction for the surface was made, implying existing only three types of surfaces: first year ice, multiyear ice and water. Under all these restrictions the brightness temperature of the Atmosphere-Ocean-Ice System T could be defined as:

$$T = T^{\uparrow} + T^{\downarrow} + T_S \quad (1)$$

$$T^{\uparrow} = \frac{1}{\cos\theta}\int_0^{\infty} T(h)\alpha_{\nu}(h)\exp(-\frac{1}{\cos\theta}\int_h^{\infty}\alpha_{\nu}(h')dh')dh \quad (2)$$

$$T^{\downarrow} = e^{-\tau}\cdot\frac{1}{\cos\theta}\int_0^{\infty} T(h)\alpha_{\nu}(h)\exp(-\frac{1}{\cos\theta}\int_0^{h}\alpha_{\nu}(h')dh')dh \quad (3)$$

$$T_S = ((C_F\cdot\varepsilon_F + C_M\cdot\varepsilon_M)\cdot T_{ice} + C_W\cdot\varepsilon_W\cdot T_W)\cdot e^{-\tau} \quad (4)$$

Where τ – atmospheric optical depth, α - atmospheric absorption coefficient, ε_F, ε_M, ε_W,- emission coefficients of First Year ice with concentration C_F, Multiyear ice (C_M) and water (C_W) correspondingly. *T(h)* is a profile of atmospheric temperature, T_{ice} and T_W refer to ice and water temperatures correspondingly. The second and third formulas define upwelling and downwelling atmospheric brightness temperatures, and the forth – surface brightness temperatures. The following models of microwave radiation - environmental medium interaction (absorption and water emission coefficients) were taken: oxygen and water vapor absorption model – Liebe, 1993; for 20 – 24 GHz water vapor absorption – Cruz Pol, 1999; ocean water dielectric permittivity – Meissner and Wentz, 2004; ocean emission coefficient dependency on surface wind speed - Aziz et al, 2005.

2) Data

The following 5 kinds of data were used to calculate SSM/I brightness temperatures: meteorological parameter profiles, sea ice temperatures, cloud data, ice concentrations, and ice emissivities.

Era-40 Reanalysis data were used both for atmospheric parameter profiles and for sea ice temperatures. The data on cloud liquid water content and cloud boundaries were modeled basing on the results of Arctic SHEBA experiment (Intrieri et al., 2002; Lin et al., 2003). Ice concentrations were set up artificially from 0 up to 1 assuming existing only three surfaces: first year ice, multiyear ice and open water. Sea ice emissivity values were not modeled, but set up and varied in the range of their natural variability, presented in Table I.

TABLE I. RANGE OF FIRST YEAR AND MULTIYEAR ICE EMISSIVITIES

		First-year ice	Dry multiyear ice
19 GHz	V	0.941±0.019	0.850±0.068
	H	0.888±0.019	0.780±0.080
22 GHz	V	0.960±0.019	0.787±0.080
37 GHz	V	0.955±0.015	0.764±0.079
	H	0.913±0.013	0.706±0.115
85 GHz	V	0.926±0.045	0.680±0.105
	H	0.886±0.031	0.650±0.011

3) Weather Filter

Weather filter, basing on numerical simulation of the ice free system, was defined. For this the brightness temperatures were selected for the cases when C_W was equal 1, and gradient ratios were calculated. It was found that for ice free ocean GR3719 should be greater than 0.054, and GR2219 should be greater than 0.015, where GR3719 = (T37V-T19V)/ (T37V+T19V) and GR2219 = (T22V-T19V)/ (T22V+T19V). TNV,H is the brightness temperature at frequency N and vertical (V) or horizontal (H) polarization.

Inverse Problem Solution

The result of numerical calculations was an ensemble of data combinations, each of them consisting of the vector of SSM/I simulated brightness temperatures and the vector of three ice concentrations: C_F, C_M and C_W. For the inverse problem solution each calculated brightness temperature was summarized with radiometric noise, normally distributed. Then the whole data set was divided into two subsets: training and testing. Each of them consisted of approximately 10000 data combinations. Training data set was used to train Neural Networks, testing – to optimize training and to calculate theoretical retrieval errors.

1) Neural Networks

Neural Networks present a general mathematical approach for the solution of different kinds of tasks including the remote sensing tasks of the best approximation (Hornik, 1991). The main advantages of NNs as a general nonlinear approximator are that they can approximate any non-linear dependencies, don't require setting up the type of the dependency between brightness temperature and ice concentrtations in advance, relatively not sensitive to noise in brightness temperatures, and ensure reasonable retrieval errors in wider range of weather conditions than traditional algorithms.

At the same time NNs have all the shortcomings of regression algorithms: their performance strongly depends upon the characteristics of the dataset used for training; the inverse function hardly can be physically interpreted; they tend to be overtuned with loss of generalization features.

2) Algorithms

In this study standard NNs of multilayer perceptron (MLP)

type with a single hidden layer of neurons and feedforward backpropagation of errors was used. Single output parameter configuration was explored: two different NNs were trained for total and multiyear ice concentrations. Optimal number of neurons was searched for both algorithms for optimization of the results (NNs complexity had been increased until the retrieval error, calculated using the testing data set started growing up)

5 input data combinations were tested with and without noise additions: 1. T19H, T19V, T22V, T37H, T37V, T85H, T85V; 2. T19H, T19V, T22V, T37H, T37V; 3. T19V, T22V, T37V, T85V; 4. T85H and T85V; 5. T19V and T37V. Here T19H, T19V, T22V, T37H, T37V, T85H, and T85V denote the brightness temperatures calculated at the corresponding frequencies and polarization (V – vertical, H - horizontal). It was found, that when no noise was added to brightness temperatures, the first combination with all SSM/I channels used ensured the smallest retrieval error. But when radiometric noise had been added to input brightness temperature values, the second combination – without high frequency channels – proved to be the best one. Both for total and for multiyear ice concentration retrieval the optimum number of neurons was 5. The optimal NNs scheme for multiyear ice concentration (C_M) retrievals is presented in Fig.1.

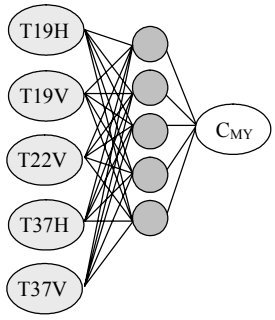

Fig.1. Optimal Neural Networks scheme for multiyear ice concentration (C_M) retrievals

For total ice concentration (C_T) retrievals the scheme is the same, but NNs weights are different. In parallel, to investigate other inversion functions beside NNs, linear multiple regression (LR) and non-liner logarithmic multiple regression (NR) coefficients were found and these regression algorithms were applied to the same testing data set.

III. Results

The results of NNs-based and other regression (MR and NR) algorithm application to testing data set are summarized in Table II and III, where the root mean square errors σ are presented for the case when no noise was added to brightness temperatures (Table II) and for noisy (normally distributed with 0.3K standard deviation) data (Table III). The left column number denotes the input channel combination number defined in the previous section.

TABLE II. ROOT MEAN SQUARE ERRORS σ, CALCULATED ON TESTING DATA SET, FOR NN, MR AND NR ALGORITHM PERFORMANCE FOR DIFFERENT INPUT CHANNEL COMBINATIONS WITHOUT NOISE ADDITION TO BRIGHTNESS TEMPERATURES.

	σ, %					
	C_T			C_M		
	NN	MR	NR	NN	MR	NR
1	1.5	1.6	3.9	0.9	1.5	3.8
2	1.4	2.2	4.1	1.3	4.2	4.0
3	3.4	5.1	7.8	5.1	8.8	9.3
4	10.3	11.3	10.0	11.6	12.9	12.9
5	4.7	5.0	7.7	11.7	12.7	14.1

TABLE III. ROOT MEAN SQUARE ERRORS σ, CALCULATED ON TESTING DATA SET, FOR NN, MR AND NR ALGORITHM PERFORMANCE FOR DIFFERENT INPUT CHANNEL COMBINATIONS WITH NOISE 0.3K, ADDED TO BRIGHTNESS TEMPERATURES.

	σ, %					
	C_T			C_M		
	NN	MR	NR	NN	MR	NR
1	1.6	2.2	4.0	3.1	5.3	5.0
2	1.7	2.3	4.3	4.1	6.3	6.2
3	3.8	5.3	8.0	7.1	9.6	10.2
4	10.0	11.3	10.1	11.6	12.9	12.9
5	4.9	5.3	8.0	11.7	12.8	14.2

It can be concluded from these tables that NNs outperform all the other regressions in all the cases. This confirms their best approximation properties. The second conclusion can be made concerning the choice of the input SSM/I channel combinations for the retrievals. It is seen that when no noise is added to the input data, use of all channels provide the best results both for total and multiyear ice concentration retrievals. But in case noise is added the retrieval error for the second combination starts to be comparable with the first one. Since noise in data may be caused by many factors, it should be considered in the most general, not only radiometric sense. Usage of high frequency channels brings not additional information but mostly additional noise into the input data which leads to abrupt increase in retrieval error.

The general conclusion is that for both C_M and C_T retrievals 5 lower SSM/I channels should be used. The theoretical retrieval errors for NNs algorithms, constitute ~ 2% for C_T and 4% for C_M retrievals.

IV. Validation

The first validation results were obtained for stable winter conditions. NNs-based algorithms were applied to SSM/I swath data for January, taken from Global Hydrology Resource Center (http://ghrc.msfc.nasa.gov/). Simultaneously SAR images were interpreted by ice expert: ice edge was derived, which was then compared with total ice concentration

field, built with NNs algorithm from SSM/I measurement data. The area of 80-90% MY ice concentration was derived from visual expert interpretation of SAR images. This was compared with MY ice concentration field, built with NNs algorithm from SSM/I measurement data.

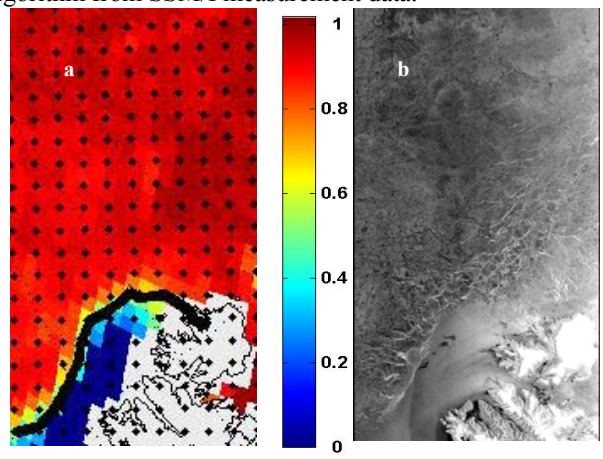

Fig. 2. Total ice concentration field (a), built from SSM/I 29 January 2008 at 06:45 UTC with NNs-algorithm with ice edge (black line) detected by expert from Envisat ASAR and Envisat ASAR calibrated image taken 29 January 2008 at 10:50 UTC

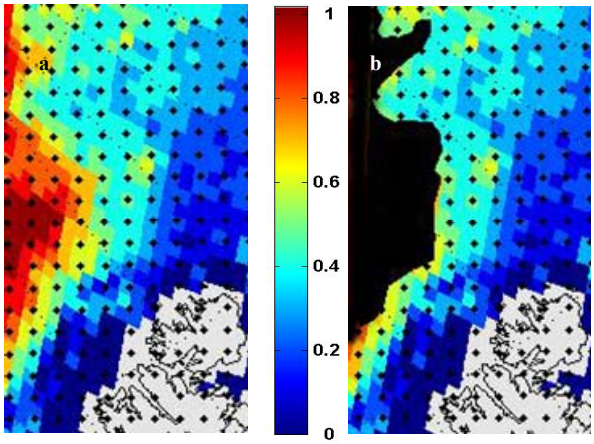

Fig. 3. Multiyear ice concentration field, built from SSM/I 29 January 2008 at 06:45 UTC with NNs-algorithm (a) and the same field with polygon of 80-100% MY ice concentration, derived by expert from Envisat ASAR image (black area) detected by expert from Envisat ASAR calibrated image taken 29 January 2008 at 10:50 UTC

In Fig. 2 and 3 the results of these comparisons for one validation case are presented. Several like cases were considered. Though such comparison is mostly qualitative, they allow to conclude that the developed algorithms behave adequately under stable winter conditions without melting (validation was fulfilled only for such cases). The ice edge, derived by expert from SAR image (Fig. 2), totally corresponds to the ice edge indicated by SSM/I NNs-retrieved C_T. The same correspondence is observed in Fig. 3 for the area of 80-90% MY ice concentration, derived from SAR and SSM/I. Further work is needed to expand the algorithms not only for stable winter conditions but also for other, more complicated systems. It needs first of all obtaining reliable values for ice emissivities and new algorithm training.

ACKNOWLEDGMENT

This work was fulfilled in the frame of integrated project "Developing Arctic Modelling and Observing Capabilities for Longterm Environment Studies (DAMOCLES) Extension". Contract 045928 (extension to contract 018509).

REFERENCES

[1] M. A. Aziz, S. C. Reising, W. E. Asher, L. A. Rose, P. W. Gaiser, and K. A. Horgan, "Effects of Air–Sea Interaction Parameters on Ocean Surface Microwave Emission at 10 and 37 GHz", *IEEE Trans. on Geosc. and Rem. Sens.*, vol.43, pp.1763-1774, 2005

[2] D. Cavalieri, "A passive microwave technique for mapping new and young sea ice in seasonal sea ice zones", *J. Geophys. Res.*, vol. 99, pp. 12561-12572, 1994

[3] J. C. Comiso, "SSMI ice concentrations using the Bootstrap Algorithm", NASA RP 1380, 50 p,1995.

[4] J.C. Comiso, and C.L. Parkinson, "Satellite observed changes in the Arctic", *Phys. Today*, vol. 57, pp. 38-44, 2004

[5] S. L. Cruz Pol, C. S. Ruf, and S. J. Keihm, "Improved 20- to 32-GHz atmospheric absorption model", *Radio Sci.*, vol. 33, pp. 1319–1333, 1998

[6] K. Hornik, "Approximation Capabilities of Mulilayer Feedforward Network", *Neural Networks,* vol. 4, pp. 251 – 257, 1991

[7] J. M. Intrieri, M. D. Shupe, T. Uttal, and B. J. McCarty, "An annual cycle of Arctic cloud characteristics observed by radar and lidar at SHEBA", *J. Geophys. Res.*, 107(C10), 8030, 10.1029/2000JC000423, 2002

[8] H. J. Liebe, G. A. Hufford, and M.G. Cotton, "Propagation modeling of moist air and suspended water/ice particle at frequencies below 1000 GHz". *In AGARD Conf. Proc.*, 542, 3.1–3.10, May 1993,

[9] B. Lin, P. Minnis, and A. Fan, "Cloud liquid water path variations with temperature observed during the Surface Heat Budget of the Arctic Ocean (SHEBA) experiment", *J. Geophys. Res.*, 108(D14), 4427, doi:10.1029/2002JD002851, 2003

[10] T. Markus, and D. J. Cavalieri, "An enhancement of the NASA Team sea ice algorithm", *IEEE Trans. Geosci. and Remote Sensing*, vol. 38, pp. 1387-1398, 2000.

[11] T. Meissner, and F.J. Wentz, "The complex dielectric constant of pure and sea water from microwave satellite observations*", IEEE Trans. on Geosc. and Rem. Sens.*, vol. 42, pp. 1836–1849, 2004

[12] E. Svendsen, K. Kloster, B. Farrelly, O. M. Johannessen, J. A. Johannessen, W. J. Campbell, P. Gloersen, D. J. Cavalieri, and C. Matzler, "Norwegian Remote Sensing Experiment: Evaluation of the Nimbus 7 Scanning multichannel microwave radiometer for sea ice research", *J. Geophys. Res.*, vol. 88, pp. 2781-2792, 1983

[13] C. T. Swift, L. S. Fedor, and R. O. Ramseier, "An algorithm to measure sea ice concentration with microwave radiometers", *J. Geophys. Res.*, vol. 90, pp. 1087-1099, 1985

[14] H. J. Zwally, J. C. Comiso, C. L. Parkinson, W. J. Campbell, F. D. Carsey, F.D., and P. Gloersen, "Antarctic sea ice, 1973-1976: satellite passive microwave observations", NASA SP-459, 1983.